Cystic Fibrosis Mucus Model to Design More Efficient Drug Therapies

(Article begins on next page)

13 July 2024

Cystic fibrosis mucus model to design more efficient drug therapies

Cosmin Butnarasu *a, Giulia Caron a, Daniela Pacheco b,c, Paola Petrini b, Sonja Visentin a

a University of Torino, Department of Molecular Biotechnology and Health Science, Via Quarello15, 10135 Torino, Italy

b Department of Chemistry, Materials and Chemical Engineering, Giulio Natta-Politecnico di Milano, Italy

c Bac3Gel Lda, TagusPark – Edificio Inovacao II, Lisbon, Portugal.

Corresponding author: cosminstefan.butnarasu@unito.it,

Abstract

Mucus can represent a strong barrier to tackle for oral or pulmonary administered drugs especially in mucus-related disorders. Still little is known about the molecular properties that mediate the interaction of drugs with mucus. This study uses a pathological cystic fibrosis (CF) mucus model to investigate the impact of mucus over the permeability of 45 commercial drugs. An *in vitro* mucosal surface was recreated by coupling the mucus model to 96-well permeable supports pre-coated with structured layers of phospholipids (PAMPA). The mucus model behaved as an interactive filter as different molecular structures reacted differently to mucus. We also found that permeability can be enhanced when calcium salts are formed. This was confirmed also through the use of cystic fibrosis sputum as a rough ex vivo model of CF mucus. Since development of drugs is characterized by a high rate of failure, the mucus platform could aid to reduce at an early stage the number of poor performer drug candidates preventing them to uselessly reach preclinical trials.

1. Introduction

The mucosal surfaces of the human body are constantly exposed to environmental threats. To counteract potential noxious agents, all the wet epithelia are covered with a layer of mucus. Mucus is a dynamic semipermeable network with a heterogeneous composition. It consists of ~95% water and the remaining 5% comprising electrolytes, lipids, DNA fragments and proteins. Maintaining the gel-like properties and keeping together such a huge amount of water requires a strong yet flexible skeleton. The tough job is carried out by mucins. Mucins are long polymeric glycoproteins having high molecular weight, consisting of a peptide backbone to which a huge amount of carbohydrate chains are attached. Such an architecture enables the exchange of nutrients, water, gases and hormones whilst being impermeable to most bacteria and pathogens [1,2].

A delicate balance of mucus production must be achieved as weakening of the mucus barrier makes us more vulnerable to environmental threats. On the contrary, an overproduction or dysfunctional clearance of mucus are hallmarks of the pathogenesis of all the mucus-related pathologies, especially pulmonary diseases[3], such as cystic fibrosis (CF) among others. In these disorders, an overexpression of mucins, accumulation of extracellular DNA as well cellular debris, and the persistent presence of bacteria, confers mucus stasis lending to a vicious cycle of infection and inflammation that can be chronically sustained [4,5]. In CF and bronchiectasis, sputum production is not only a daily reality, but also a crucial marker for physicians during both stable state and exacerbation used to evaluate disease severity and treatment response. Sputum's reliability as an indicator of disease has led it to being proposed as an important clinical prognostic factor in mucus-related diseases. This has been taken a step further by Murray and colleagues, who explored the utility of sputum color in patients with bronchiectasis by developing a quantitative method that predicts bacterial colonization based on the color of sputum [6].

Despite the great advancements in disease management of the last decades, pulmonary failure remains the main cause of morbidity and mortality in patients with CF. The lack of function of the cystic fibrosis transmembrane conductance regulator protein (CFTR) in people with CF, leads to mucus dehydration. As a result, mucus undergoes a reduced clearance, clogging the airways and making it difficult to breath. Physicians have developed advanced clearance techniques (ACTs) based on coughing maneuvers to get rid of the viscous mucus. In addition to the routinely ACTs, CF patients manage their disease by following a regular treatment with medications. The recurrent pulmonary

67 exacerbations are usually treated with both oral and intravenous antibiotics (*i.e.*,
68 aztreonam, tobramycin, levofloxacin), and anti-inflammatory drugs (*i.e.*, high-doses
69 ibuprofen [7]).

70 Yet, to enter into the systemic circulation, drugs administered by the oral, pulmonary,
71 nasal or rectal routes, need come in contact and subsequently cross the epithelium in
72 order to reach the capillary circuitry in the lamina propria. Thus, effective drugs
73 administered by these routs should harbor the ability to transverse mucus barriers to
74 be pharmacologically active. In the context of cystic fibrosis, the pathological mucus can
75 strongly limit the absorption of drugs that do not exhibit these difficulties under normal
76 physiological conditions. Also, the pathological CF mucus, is characterized by a reduced
77 mesh size (60-300 nm)[8] with respect to physiological mucus (497-503 nm)[9]. Two main
78 mechanisms are expected to affect drug diffusion through mucus: steric and interactive
79 filtering (Fig. 1). Oligomers of secreted mucins connect with each other creating a
80 complex network that filters molecules bigger than the size of the mesh spacing
81 between mucin fibers [10] (steric filter). Molecules small enough to penetrate the mucin
82 mesh are subjected to the interactive filter which is mainly governed by the structural
83 complexity of mucins. On the highly glycosylated hydrophilic regions, negative charges
84 are exposed due to the presence of sialic acid. On these substrates, hydrogen bonding
85 and electrostatic interactions can be established with polar and hydrophilic molecules.
86 But not the entire peptide core of mucins is glycosylated; cysteine-rich domains are
87 glycans free and usually folds into hydrophobic regions on which lipophilic molecules
88 can attach. And yet, mucin is just one of the components of mucus. Other substances
89 such as lipids, antimicrobial peptides (defensins, histatins, collectins *etc.*,), lytic
90 enzymes (lysozyme) and antibodies (IgA and IgG) are components of mucus as well,
91 and each one of them has the potential to interact with drugs.

92
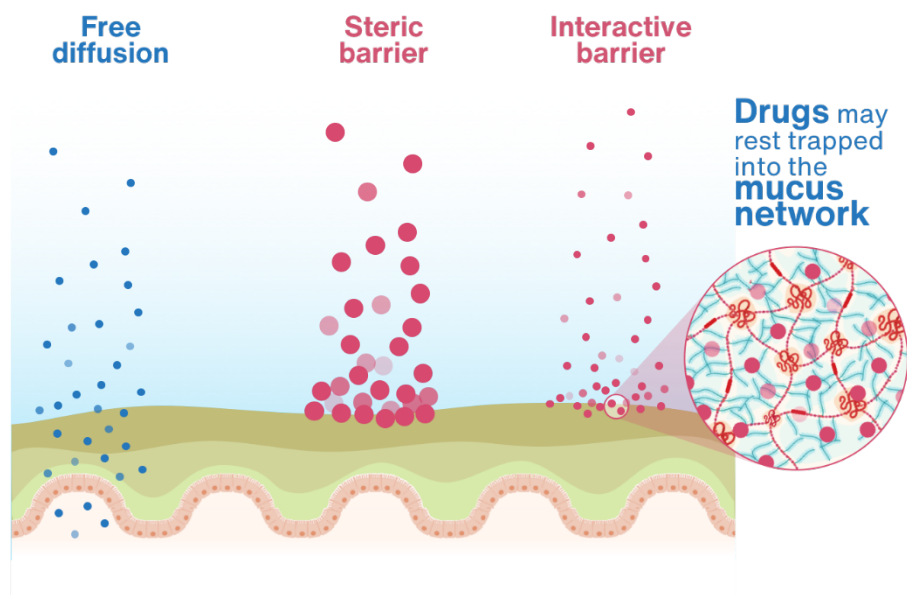
Figure 1. The steric and interactive barriers of mucus. Drugs larger than the mesh spacing between mucin fibers are stacked within mucus because too big to cross the mucus mesh. Similarly, drugs smaller than the mesh but able to interact with mucus components are equally retained by mucus. On the contrary, particles that are small enough and relatively inert to any of the mucus component can freely diffuse through the mucus layer and eventually absorbed.

The importance of developing *in vitro* models able to model both the biological structure and functions of pulmonary mucus is increasingly gaining awareness in modern drug discovery. Today, the most popular *in vitro* models for assessing permeability/absorption of drugs, are those based on artificial membranes, such as parallel artificial membrane permeability assay (PAMPA) [11], systems based on cells, such as Caco-2 [12] and MDCK [13]; and systems based on site-specific tissues [14]. Notably, none of them takes mucus specifically into account. In the last years, a variety of mucus models have been proposed [15]. The proposed models include gastrointestinal mucin-based solutions[16,17], reconstituted oral mucus gels [18], multilayered polyelectrolyte films [19], and *in vitro* cell cultures models incorporating airway mucus or mucus-producing cells [20]. Falavigna *et al.* developed a mucus phospholipid vesicle-based permeation assay that has been used for permeability screening of drugs and formulations [21].

Recently we developed an *in vitro* mucus model which simplifies mucus complexity by mimicking the chemical composition, structural features and viscoelastic properties of pathological CF mucus [22]. The viscoelastic property of CF mucus is achieved by taking advantage of the internal gelation of alginate in the presence of calcium ions. Alginate is an extracellular exopolysaccharide component of mucoid *P. aeruginosa*, a hallmark of CF infection, and has been shown to protect bacteria against certain antibiotics as well

118 as escape the immune system [23,24]. To reproduce the interactive and steric filters of CF
119 mucus we used commercially available unpurified mucin type III from porcine stomach.
120 One may argue that commercial mucins are different in terms of structure and
121 viscoelastic properties respect to native mucins. Indeed, it has been established that
122 commercial mucins fail to form hydrogels at acidic pH, are only partially purified and
123 are inferior in inhibiting virus infection compared to natively purified mucins obtained
124 in lab [25]. However, the purpose of our mucus model is to have an easy to use and easy
125 to reproduce *in vitro* mucus model suitable for average throughput screening (HTS)
126 applications. Thus, even if in lab extracted mucins are qualitatively superior to
127 commercial mucins, the time consuming and expensive procedures of purification,
128 extraction and concentration at laboratory level are not adapted for HTS purposes.
129 In this study, we aimed at expanding the applicability and relevance of our *in vitro* cystic
130 fibrosis pathological mucus model. To reach this aim we addressed the following goals:
131 (i) selected 45 commercially available drugs maximizing physicochemical variability;
132 (ii) performed PAMPA measurements in the absence of mucus and assessed the
133 physicochemical determinants of apparent permeability (P_{app}); (iii) we coupled the
134 developed mucus model with PAMPA to mimic *in vitro* cystic fibrosis airway mucosal
135 surface. The permeability in the presence of mucus was compared with the P_{app}
136 obtained in the absence of mucus; (iv) eventually, permeability with cystic fibrosis
137 sputum was measured to support the conclusion drawn from the *in vitro* model herein
138 presented.
139 Overall, this study highlights the challenging of reproducing *in vitro* the complexity of
140 cystic fibrosis dysfunctional mucus. While PAMPA could be a reasonable model to
141 mimic permeability through cellular membrane, we have shown that it is a too
142 simplistic model to mimic the diffusion across pathological CF mucus. As a first
143 screening tool of poorly permeable molecules, a fully tunable in vitro mucus model,
144 easy to reproduce, and mimicking both the composition and the rheological properties
145 of CF mucus, could be of high usefulness in the early drug discovery.
146
147 **2. Experimental section**
148
149 **2.1. Computational Part**
150 The drug SMILES codes were retrieved from DrugBank [26]. The csv file of the approved
151 drugs was downloaded from DrugBank (last update on 3 January 2021). The csv file
152 was transformed in xlsx file using Microsoft Excel (v. 16.43). The SMILES of CFTR$_{inh}$-
153 172, which is a non-commercial drug acting as an inhibitor of the CFTR protein, was

5

154 retrieved from PubChem[27]. Molecular properties were calculated with DataWarrior
155 (ver. 5.5.0, openmolecules.org) and include physico-chemical properties, druglikeness
156 related properties, various atom and ring counts, molecular shape, flexibility as well as
157 functional groups (Table S2). The molecular charge at pH 7.4 was retrieved from
158 MarvinSketch (Marvin 20.20, 2020, ChemAxon).

159 The dataset was analyzed with the Principal Component Analysis (PCA) tool
160 implemented in DataWarrior. The correlation matrix of the descriptors was calculated
161 using DataWarrior and represented as a heatmap.

162

163 ## 2.2. Materials

164 Mucin from porcine stomach (PGM Type III, bound sialic acid 0.5-1.5%, partially
165 purified powder), sodium salt of alginic acid, calcium carbonate, D-(+)-gluconic acid δ-
166 lactone ≥99.0% and sodium chloride used to develop the airway mucus model were all
167 purchased from Merck (Germany). Permeability experiments were carried out on
168 Corning® Gentest™ Pre-coated PAMPA, 353015, USA plates. Millipore® grade water
169 (resistivity: 18.2 MΩ cm at 25 °C) was obtained from an in-house Millipore® system.
170 Acetonitrile, ammonium acetate and DMSO were of the highest available grade and
171 purchased from Sigma Aldrich. The drugs used in this study were all commercially
172 available (Fig. S1). Stock solutions were prepared in DMSO and stored at 4 °C.

173

174 ## 2.3. Mucus model

175 The herein used mucus model can be exploited as a platform for drug diffusion either
176 for cystic fibrosis mucus or other mucus-related disorders such as mucus of chronic
177 obstructive pulmonary disease, which unveils its potential for a wide range of
178 applications in drug discovery. The mucus model was prepared as previously described
179 [22]. Briefly, a 21 mg/mL alginate sodium salt solution was dissolved in a 16.3 mg/mL
180 NaCl solution, under slow magnetic agitation. In parallel, a 43.7 mg/mL mucin
181 suspension was prepared in mQ water and left under slow agitation over-night. The
182 alginate and mucin solutions were mixed at a 1:4 proportion using two jointed luer-
183 lock syringes. Then, the alginate and mucin suspension were mixed with a suspension
184 of 7 mg/mL $CaCO_3$ prepared in 16.3 mg/mL NaCl solution. In the last step, a 70 mg/mL
185 GDL solution was freshly prepared in 16.3 mg/mL NaCl and mixed with the previously
186 prepared suspension (alginate, mucin and $CaCO_3$) at a proportion of 1:6. Finally, 40 μL
187 of the mucus model were pipetted directly over the PAMPA membrane in the donor
188 compartment, producing a hydrogel of approximately 500 μm in thickness. The donor
189 plate of the PAMPA was then carefully shacked to uniformly distribute the volume of

mucus over the entire well surface and to get rid of any air bubbles. Afterwards, the mucus within the plate was left to crosslink for 24 h before the addition of drug solutions. Throughout the time course of the permeability experiment, the CF mucus model remained stable with respect to weight and thickness variations. In fact, we previously determined that after 6h of incubation in an aqueous medium, mucus undergoes a thickness variation below 10% which was considered acceptable for our experimental purpose[22].

2.4. PAMPA assay

The apparent permeability (P_{app}) and the effect of mucus on permeability were experimentally determined through PAMPA and mucus-PAMPA assays, respectively. Stock solutions of all drugs were prepared in DMSO at a concentration of 10 mg/mL. Donor solutions of drugs were prepared in PBS (10 mM, pH 7.4, 5% DMSO) at a concentration between 100 to 500 μM, depending on the drugs' specific solubility. Each donor well was filled with 200 μL of drug solution, while the acceptor wells were filled with 300 μL of PBS. The donor plate was then placed on top of the acceptor plate, so the artificial membrane was in contact with the buffer solution below. A lid was placed on top of the donor plate and the whole PAMPA plate was incubated at room temperature for 5 h. At the end of the incubation period, the plates were separated, and the volume of the acceptor wells was collected. Concentrations of drugs in each acceptor well were quantified either by HPLC-UV or HPLC-MS. The apparent permeability coefficient (P_{app}) was expressed using equation 1 derived from Fick's law[28] for steady state conditions:

$$P_{app} = \frac{dQ/dt}{C_0 \times A} \qquad (Eq.\,1)$$

where dQ is the quantity of drug expressed as moles permeated into acceptor compartment at time t (18,000 sec), C_0 is the initial concentration in the donor well and A is the area of the well membrane (0.3 cm^2). The P_{app} was used as an average of all the measures.

The same PAMPA experimental setup was adopted when assessing the effect of individual components of mucus. In particular, we evaluated how the PGM, the NaCl, the alginate hydrogel and calcium impact on permeability. For this purpose, the passive diffusion was measured in the presence of each one of these chemicals. Each of which, were individually added in the donor compartment of the PAMPA. In brief, 40 μL of the alginate gel were deposited over the phospholipid membrane of the donor compartment prior the addition of drug solution. The influence of PGM was assessed by filling the donors with a suspension of drug containing 4.16 mg/mL of PGM (the PGM concentration donor compartment). Similarly, drug donor solutions containing 1.67

226 mM CaCl$_2$ or 20 mM NaCl were used when investigating the impact of calcium and NaCl
227 over permeability.

228

229 **2.5. Cystic fibrosis sputum**

230 Sputum collected from cystic fibrosis patients was used as a model of complex
231 biological matrix representative of CF mucus. We measured the permeability of some
232 of the drugs of our dataset using the CF sputum – PAMPA system and compared the
233 results with the permeability obtained in the presence of our mucus model. Sputum
234 samples were a kind concession of Prof. A. Ghigo from the Department of Molecular
235 Biotechnology of University of Turin. Spontaneously expectorated sputum was
236 collected into sterile containers and was processed as described by Oriano *et al.* [29].
237 Briefly, samples were processed getting first rid of saliva. Then, samples were diluted
238 8x in PBS, vortexed until sputum dissolution and centrifuged for 15 min at 3000 g. Forty
239 µL of sputum were deposited over the PAMPA membrane in the bottom of the top plate,
240 and eventually 200 µL of drug solution were inserted over the layer of CF sputum, while
241 300 µL of PBS were inserted into the bottom plate of the PAMPA. The two plates were
242 coupled and incubated for 5h. At the end of the 5h the plates were splitted and the
243 amount of drug diffused into the bottom plate was quantified. Similarly, to test the effect
244 of calcium over the permeability of the drug, we formed drug-calcium complexes by
245 dissolving the drug into PBS containing calcium at the same concentration present in
246 the cystic fibrosis mucus model. The permeability of calcium-drug complexes was
247 measured through the CF sputum PAMPA as previously described.

248

249 **2.6. Quantification**

250 All compounds, except ebselen, benzoic acid and 3-aminophenol, were analyzed and
251 quantified by HPLC-MS/MS using a Varian HPLC equipped with a 410 autosampler and
252 an Ascentis C18 column (10 cm x 2.1 mm, 3 µm). Gradient mobile phases composed of
253 acetonitrile and water 0.1% formic acid or ammonium acetate 5 mM pH 6.6 as organic
254 and aqueous phase respectively were pumped at a flow rate of 200 µL/min. A flow of
255 200 µL/min and an injection volume of 10 µL were used. Compounds were detected on
256 a Varian 320 MS TQ Mass Spectrometer equipped with an electrospray ionization (ESI)
257 source operating in positive or negative mode, depending on drugs' method. The
258 detector was used in multiple reaction monitoring (MRM) mode and the transitions of
259 each drug are reported in Table S1.

260 Ebselen, benzoic acid and 3-aminophenol were quantified on a HPLC Varian ProStar
261 equipped with a 410 autosampler and a PDA 335 LC Detector. The analysis was

262   conducted on a IAM column (Regis, 10 cm x 4.6 cm 10 μm packing 300 Å pore size)

263   using ammonium acetate and acetonitrile as aqueous and organic mobile phase,

264   respectively. The flow rate was 1 mL/min.

265

266   **2.7. Statistical analysis**

267   A minimum of 4 replicates were conducted for each compound on each experimental

268   method (with or without the mucus model), some of whom repeated also on different

269   PAMPA plates. Results are expressed as mean ± SD. Student's t-test was applied to

270   detect statistical significance between the permeability recorded with and without

271   mucus. A $p<0.05$ was considered to be a statistically significant difference.
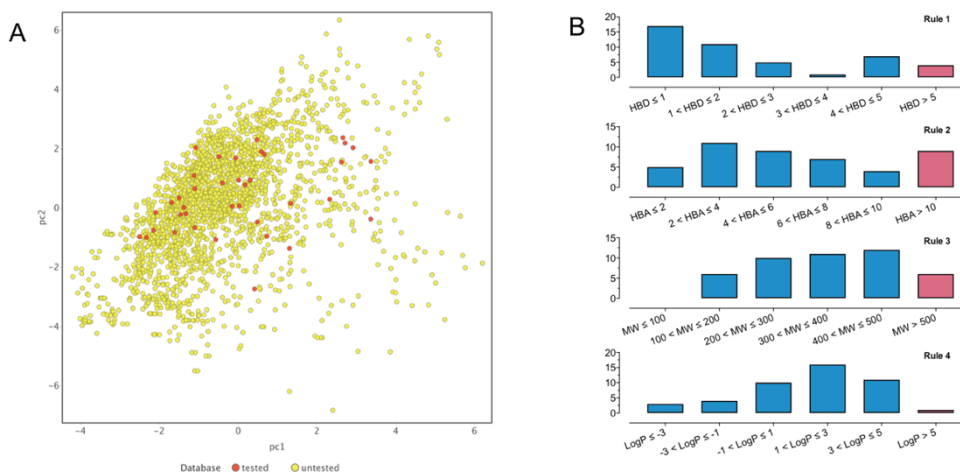
272

273   **3.   Results and discussion**

274

275   **3.1. Dataset selection: assessment of chemical heterogeneity**

276   We included in our dataset a number of anti-inflammatory (ibuprofen, dexamethasone)

277   and antibacterial drugs (tobramycin, ceftazidime, aztreonam, ciprofloxacin,

278   tetracycline) commonly employed in the cystic fibrosis therapy regimes. To properly

279   evaluate the performances of our CF mucus model, we expanded the dataset up to 45

280   compounds considering it a reasonable number of drugs to be investigated, with good

281   variability in terms of chemical properties (see below).

282   To assess the distribution of our dataset within the entire drug chemical space, at first,

283   we downloaded the DrugBank database of approved drugs. From DrugBank's database

284   we retrieved the SMILES code for each compound and used them to calculate molecular

285   descriptors (see Methods, Table S2). Using drugs as observations and the selected

286   molecular descriptors as variables, we then computed a principal component analysis

287   (PCA). The drugs within our dataset are small molecules therefore, focus was pointed

288   on compounds of total molecular weight <1,000 Da (yellow dots in Fig. 2A). The

289   variance explained by PC1 and PC2 using 30 molecular descriptors is about 60%. In the

290   score plot defined by PC1 and PC2 is possible to appreciate a good distribution of the

291   tested drugs within the chemical space (red dots in Fig 2A).

292   To assess chemical variability within our dataset we also evaluated the Lipinski's rule

293   of five (Ro5) molecular descriptors distribution (the number of the hydrogen bond

294   donors (HBD), the number of the hydrogen bond acceptors (HBA), the molecular mass

295   (MW), and the octanol-water partition coefficient (LogP)). Figure 2B shows that all the

296   descriptors categories are well represented by the dataset,

297

Figure 2. (A) Distribution of the tested drugs (red dots) within the DrugBank database of approved drugs (yellow dots) having total molecular weight ≤1000 Da. (B) Classification and distribution based on Lipinski's rule of five (B). Compounds that violate the Ro5 for each molecular descriptor are represented by the red bars.

3.2. Validation of the permeability setup to measure P_{app}

Before evaluating the effect of mucus on drug permeability, we determined and validated permeability in the absence of mucus through an artificial cellular membrane since our method differs from the standard PAMPA protocol. In fact. in our setup (modified setup), mucus was placed over the PAMPA membrane (a filter plate pre-coated with structured layers of phospholipids). in the top well as is the only way to have a physical support that can sustain mucus. Thus, diffusion takes place from the top to bottom well and drug has been quantified only in the acceptor compartment (bottom well).

Data obtained with our original set-up (Table 1) were firstly validated using a subset of compounds taken from the paper of Chen et al.,[30] (Table S3 and Fig. S2) using the same artificial membrane (r^2=0.610, Fig. S2) . Notably, compounds as propranolol and caffeine known for being high permeable[31,32] could clearly be discriminated from low permeable compounds.

Then we determined which molecular descriptors mostly govern permeability in our system. To do that a correlation matrix between apparent permeability (P_{app}) and a pool of molecular descriptors (Fig. S3 and Methods) were calculated. The highest correlation (r^2 = 0.303) was found to exist with topological polar surface area (TPSA, the surface sum over all polar atoms or molecules, mainly oxygen and nitrogen, also including their attached hydrogen atoms) and in minor extent with hydrogen bond donor and acceptor groups (HBD and HBA). In particular, the higher the TPSA, the lower the P_{app}. This is in line with the literature [33] and again confirms the reliability of our system.

326 Finally, we verified whether TPSA can distinguish high from low permeable
327 compounds. Although a definitive threshold is missing, in the standard PAMPA setup
328 the P_{app} value for distinguishing low from highly permeable compounds is frequently
329 set at 1.5×10^{-6} cm/s [30]. However, in a modified setup (diffusion from the top to the
330 bottom well) the permeability threshold is higher [34] [35]. Here we used 4×10^{-6} cm/s and
331 1×10^{-6} cm/s to distinguish high, medium and low permeable molecules. Figure 3B
332 shows that TPSA values of 140 $Å^2$ [36]. and of 75 $Å^2$ [37,38] are able to predict permeability
333 class of the investigated dataset.

334 In addition to the discrimination based on the total polar surface area, we plotted the
335 high and low permeable compounds in the chemical space based on their chemical
336 properties. For this purpose, we computed a principal component analysis using as
337 variables the molecular descriptors calculated from DataWarrior. Indeed, we can
338 observe a good separation of the two groups on the first principal component (See Fig.
339 S4 A-C).

340
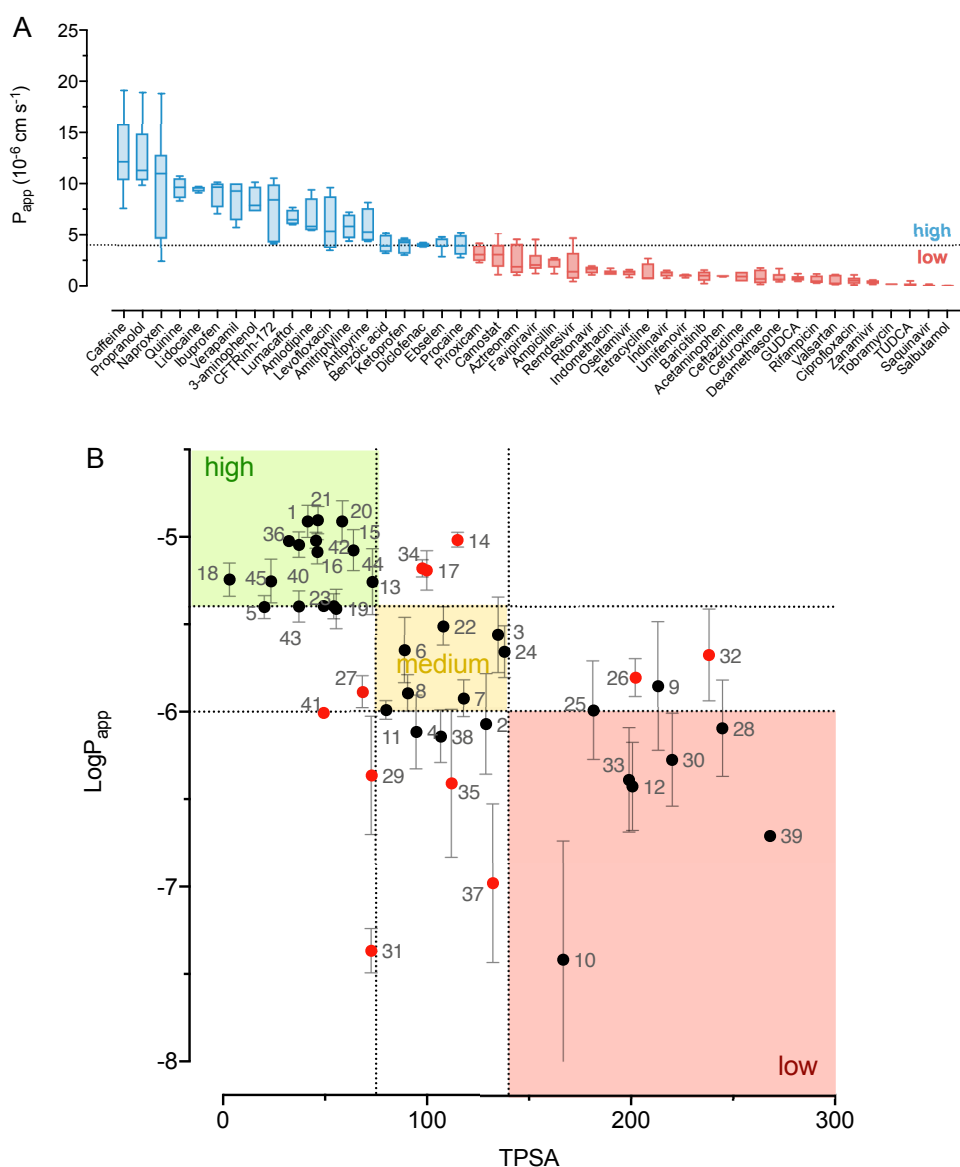
Figure 3. Classification in high and low permeable compounds (A) of the tested drugs based on the determined apparent permeability (P_{app}) Dataset grouping within permeability categories (B): permeability classification: green = high, yellow = medium, red = low. The P_{app} threshold high-medium and medium-low permeable compounds was set at 4 and 1×10^{-6}, respectively. TPSA threshold between high-medium and medium-low permeable compounds was set at 75 and 140 Å², respectively. The number beneath each dot refers to drug name (see Fig. S1 and Table 2).

Overall, we validated the goodness of the experimentally determined P_{app} in the absence of mucus and confirmed that the P_{app} values can be used as benchmark when assessing the effect of mucus in the mucus-PAMPA system.

3.3. Permeation studies in the presence of a mucus model

The mucus model was adapted to the PAMPA plate by directly pipetting it on top of the phospholipid membrane in the donor compartment. As all the wet epithelia of the human body are covered by mucus, drugs administered by oral or pulmonary routes have to cross both the mucus layer and the cellular membrane to be absorbed, and thus to be effective. With our adapted mucus-PAMPA system we are expecting to be able to mimic *in vitro* the interface at mucosal surfaces. (Fig. 4).
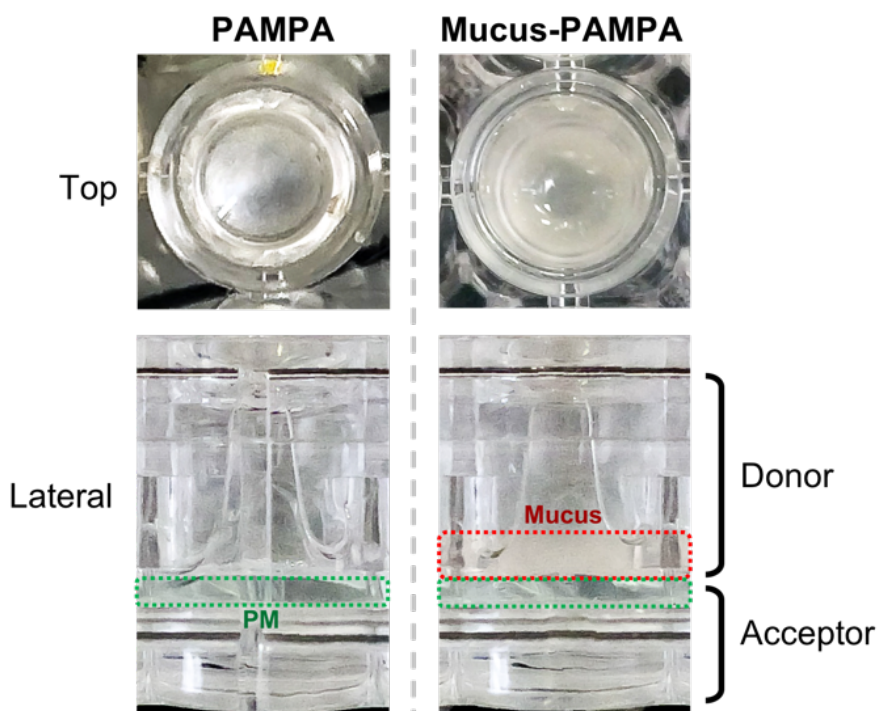
Figure 4. Comparison between PAMPA and mucus-PAMPA system. On top the upper view of the PAMPA wells, on the bottom the lateral view of the donor and acceptor compartments. Dashed lines highlight the mucus layer and the phospholipid membrane (PM).

The effect of mucus was measured in terms of variations of permeability and was considered statistically significant only if the p-value between the means of the two groups (PAMPA and mucus-PAMPA) was <0.05. A summary of the P_{app} with and without mucus is reported in Table 1, while the detail of each drug tested is reported in SI (Fig. S6).

Table 1. Summary of the P_{app} recorded on PAMPA and the effect the mucus model played over permeability with the respective P_{app} variations. The terms *increased / decreased* are used only if the difference on permeability is statistically significant. Student's t-test was applied to detect statistical significance between

the permeability recorded with and without mucus. A p<0.05 was considered to be a statistically significant

377 difference.

378

| Nr	Compound	MW (g/mol)	Lipophilicity	P_{app} PAMPA (± SD) ×10⁻⁶ [cm/s]	P_{app} Mucus-PAMPA (± SD) ×10⁻⁶ [cm/s]	Effect of mucus on P_{app}
1	Propranolol	259.3	medium	12.56 (± 2.9)	2.84 (± 1.4)	Decreased (-1)
5	Ebselen	274.2	low	4.01 (± 0.6)	1.82 (± 0.8)	Decreased (-1)
8	Oseltamivir	312.4	medium	1.30 (± 0.3)	0.32 (± 0.1)	Decreased (-1)
11	Umifenovir	477.4	medium	1.03 (± 0.1)	0.18 (± 0.0)	Decreased (-1)
12	Zanamivir	332.3	medium	0.42 (± 0.2)	0.02 (± 0.0)	Decreased (-1)
13	Levofloxacin	361.4	low	5.94 (± 2.7)	0.00 (± 0.0)	Decreased (-1)
14	CFTRinh-172	409.4	medium	7.35 (± 2.9)	3.84 (± 1.2)	Decreased (-1)
15	Verapamil	454.6	low	8.57 (± 2.0)	0.53 (± 0.5)	Decreased (-1)
16	3-aminophenol	109.1	low	8.28 (± 1.4)	0.74 (± 0.6)	Decreased (-1)
17	Amlodipine	408.9	medium	6.60 (± 1.9)	0.00 (± 0.0)	Decreased (-1)
18	Amitriptyline	277.4	high	5.80 (± 1.2)	0.00 (± 0.0)	Decreased (-1)
19	Procaine	236.3	low	4.00 (± 1.0)	0.00 (± 0.0)	Decreased (-1)
20	Caffeine	194.2	low	12.70 (± 3.5)	6.43 (± 4.2)	Decreased (-1)
25	Tetracycline	444.4	high	1.22 (± 1.0)	0.00 (± 0.0)	Decreased (-1)
26	Ritonavir	721.0	high	1.60 (± 0.4)	0.61 (± 0.2)	Decreased (-1)
31	Salbutamol	239.3	low	0.04 (± 0.0)	0.01 (± 0.0)	Decreased (-1)
34	Lumacaftor	452.4	medium	6.64 (± 0.8)	5.40 (± 0.3)	Decreased (-1)
36	Lidocaine	234.3	high	9.47 (± 0.3)	0.05 (± 0.1)	Decreased (-1)
38	GUDCA	449.6	medium	0.76 (± 0.3)	0.22 (± 0.3)	Decreased (-1)
42	Quinine	324.4	low	9.54 (± 1.0)	6.66 (± 0.6)	Decreased (-1)
3	Camostat	398.4	medium	3.04 (± 1.3)	3.28 (± 2.9)	None (0)
4	Dexamethasone	392.5	medium	0.85 (± 0.4)	0.46 (± 0.4)	None (0)
6	Favipiravir	157.1	high	2.44 (± 1.1)	3.17 (± 1.3)	None (0)
7	Indinavir	613.8	low	1.22 (± 0.3)	0.94 (± 0.7)	None (0)
9	Remdesivir	602.6	low	1.86 (± 1.6)	1.63 (± 1.5)	None (0)
10	Saquinavir	670.9	high	0.08 (± 0.1)	0.10 (± 0.1)	None (0)
24	Ampicillin	349.4	high	2.29 (± 0.6)	1.34 (± 0.7)	None (0)
28	Ceftazidime	546.6	low	0.93 (± 0.5)	1.14 (± 1.0)	None (0)
29	Ciprofloxacin	331.3	low	0.54 (± 0.3)	0.31 (± 0.3)	None (0)
30	Rifampicin	823.0	high	0.61 (± 0.4)	0.19 (± 0.1)	None (0)
32	Aztreonam	435.4	low	2.45 (± 1.5)	1.64 (± 0.6)	None (0)
33	Cefuroxime	424.4	low	0.87 (± 0.7)	0.16 (± 0.2)	None (0)
35	Valsartan	435.5	low	0.56 (± 0.5)	0.44 (± 0.5)	None (0)
37	TUDCA	499.7	high	0.17 (± 0.2)	0.04 (± 0.1)	None (0)
39	Tobramycin	467.5	high	0.19 (± 0.0)	0.25 (± 0.1)	None (0)
40	Ibuprofen	206.3	medium	9.09 (± 1.4)	10.33 (± 1.2)	None (0)
45	Antipyrine	188.2	medium	5.75 (± 1.7)	6.19 (± 2.6)	None (0)
2	Baricitinib	371.4	high	0.99 (± 0.5)	2.68 (± 2.1)	Increased (+1)
21	Naproxen	230.3	low	9.57 (± 3.9)	22.02 (± 6.1)	Increased (+1)
22	Piroxicam	331.4	high	3.15 (± 0.8)	6.63 (± 0.1)	Increased (+1)
23	Diclofenac	296.2	medium	4.03 (± 0.2)	5.06 (± 0.1)	Increased (+1)
27	Indomethacin	357.8	medium	1.32 (± 0.3)	2.54 (± 0.9)	Increased (+1)
41	Acetaminophen	151.2	medium	0.99 (± 0.1)	6.22 (± 0.9)	Increased (+1)
43	Benzoic acid	122.1	medium	4.06 (± 0.9)	9.91 (± 0.9)	Increased (+1)
44	Ketoprofen	254.3	low	4.04 (± 0.7)	9.24 (± 1.2)	Increased (+1)

379

380

381 Three kinds of mucus-induced effects were observed (Table 1 and Fig. 5A): a) in the

382 presence of mucus, 44% of drugs showed a decreased permeability, b) 38% had no

383 statistically significant variation, and c) 18% had an increased permeability. Among the

384 compounds which diffusion was reduced by mucus, we cannot outline any dependency

385 on drugs lipophilicity. In fact, mucus reduced the permeability of both hydrophilic and

386 lipophilic drugs which is in agreement with what found by Boegh *et al.*, [18] using a

387 biosimilar mucus on Caco-2 cells, and Falavigna *et al.*, [21] with a mucin-PVPA system.

388   Data suggests that the CF pathological mucus model did not act as a mere physical
389   barrier. It behaves as an interactive filter as different structures interacted differently
390   with mucus. This can be attributed to low affinity interactions taking place during the
391   diffusion process across the mucus layer and is mostly dependent on the structure of
392   mucins. In fact, due to the complex architecture of mucins, hydrophobic drugs can be
393   retained by the naked domains of the peptide core of mucin, while hydrophilic drugs
394   can entangle with the branched oligosaccharides. In addition to the interactive filter
395   orchestrated by mucins through hydrophobic, electrostatic and hydrogen bonding
396   interactions, mucins can hinder the diffusion of xenobiotics also through a size filtering
397   mechanism dependent on the mucin mesh. To estimate the mesh size of our mucus
398   model we applied the generalized Maxwell model (GMM) as described in our previous
399   work[22]. The estimated mesh size was 54.7 ± 5.35 nm which is in good agreement with
400   what reported in the literature for pathological mucus. Considering that our dataset is
401   composed of only small molecules, thus much smaller than the mesh of our mucus
402   model, we think the steric filter had a minor impact on drug diffusion.
403   Once we had assessed the effect that mucus plays on the P_{app} (*i.e.*, decreased, no effect,
404   increased) of each compound, we then wanted to quantitatively compute the activity of
405   mucus. Thus, we assigned numerical values to each effect, particularly -1, 0, +1 when
406   the permeability was decreased, unvaried and increased, respectively. The effect of
407   mucus over permeability varies without any apparent relation to any of the molecular
408   descriptors selected, as shown by the correlation matrix (Fig. S3), In fact, the relation
409   between the P_{app} and TPSA registered in the absence of mucus does not hold true
410   anymore. If we previously could correctly predict the permeability of almost 80% of the
411   tested compounds, after the addition of mucus we see that only 53% of the molecules
412   have their permeability correctly predicted (Fig. 5B). For instance, amitriptyline
413   (compound nr. 18) in the absence of mucus belongs to the high permeable group as it
414   has low TPSA and high P_{app}; in contrast, the presence of mucus strongly decreases its
415   permeability. Amitriptyline is a highly lipophilic drug though being positively charged
416   at pH 7.4. Such a reduction of permeability that we observe, may be the result of a
417   combined retention due to interactions with the lipophilic domains and the negatively
418   charged glycans of mucin. As amitriptyline, many other drugs have their permeability
419   decreased (see Table 1 and Fig. 5).
420   With the drug diffusion studies on the mucus-PAMPA system we show that the
421   pathologic cystic fibrosis mucus model can strongly influence the permeability of drugs.
422   Theoretically, if the observed effects would have been similar for all compounds, one
423   could reasonably state that the rate-limiting factor could be the longer diffusive

424 pathway when in the presence of mucus. Though, this hypothesis should be discarded

425 as we have found that for some drugs the presence of the pathological mucus model

426 may increase permeability. These results are discussed in the next session.

427
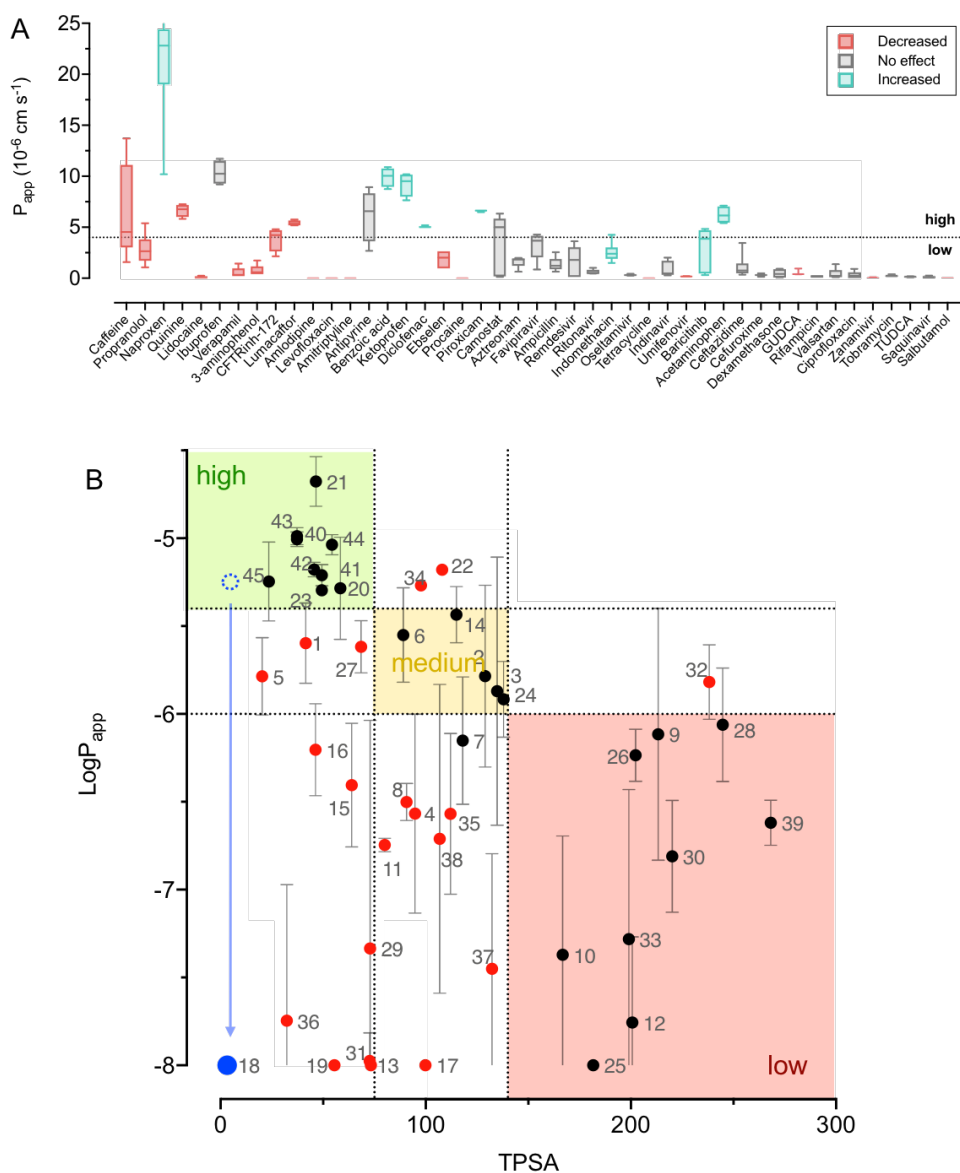
428

429 **Figure 5**. The impact of mucus over permeability. (A) The permeability recorded in the presence of mucus.

430 (B) Grouping within permeability categories of the 45 compounds tested (permeability classification: green

431 = high, yellow = medium, red = low). The P_{app} threshold of high-medium and medium-low is set at 4 and 1 $\times$

432 10^{-6}, respectively. TPSA threshold of high-medium and medium-low is set at 75 and 140 $Å^2$, respectively. The

433 number beneath each dot refers to drug name (see Fig. S1 and Table 2). As an example, focus is pointed on

434 the variation of permeability of amitriptyline (nr 18, blue dot) in the absence and presence of mucus.

435

3.4. On the increased permeability in the presence of pathological mucus

We expected the mucus model to reduce or have no effect on the permeability of drugs. Figure 5A clearly reports that some of the compounds we tested (such as naproxen) presented a higher permeability in the presence of mucus than in its absence. Among the tested drugs, 18% (baricitinib, naproxen, piroxicam, diclofenac, indomethacin, acetaminophen, benzoic acid, ketoprofen) had a significant increase of permeability in the presence of mucus. In respect to the entire dataset, the increased-permeability group share some chemical-physical properties; they are relatively small molecules (MW < 380 Da, Total Surface Area < 270 $Å^2$), lipophilic (cLogP > 1), have medium-low polarity (PSA<130 $Å^2$), and 6 out of 8 are negatively charged at pH 7.4.

3.4.1. The role of the mucus components in the enhancement of permeability

To isolate the driving force of the increased diffusion rate observed in the presence of our mucus model, we disassembled the mucus and measured the permeability of naproxen in the presence of each one of the components of mucus. For this purpose, we selected naproxen as a model drug as it is the most remarkable compound for which the permeability increases with mucus (Fig S6). The main components of our mucus model are PGM which is used to mimic the composition of CF mucus; alginate because it is produced by mucoid *P. aeruginosa* infecting the CF mucus; $CaCO_3$ used to crosslink alginate, and NaCl necessary to reproduce the salinity of CF mucus. Thus, we performed a PAMPA assay where naproxen solutions were prepared in PBS buffer containing either PGM, or NaCl or calcium in the same concentrations used in the mucus model. In the case of the alginate gel, it was deposited on the bottom of the top compartment of the PAMPA the day before the experiment to allow alginate to crosslink. (top of Fig. 6). We observed that while the diffusion rate in the presence of PGM or NaCl did not undergo major variations, in the other two systems (*i.e.*, the alginate gel and $CaCl_2$) a net increase of permeability was obtained. It is noteworthy to remind that the alginate gel contains calcium as it is necessary to crosslink the alginate solution hence, to form the hydrogel matrix. The most probable scenario explaining such an activity could rely on ion-pairing as it is known that Ca^{2+} ions have a strong affinity for O, N or F atoms because the metal act as Lewis acid and thus form complexes with many ligands [39]. The binding of calcium ions is highly selective and can form asymmetric complexes that consist of a large radius.

17
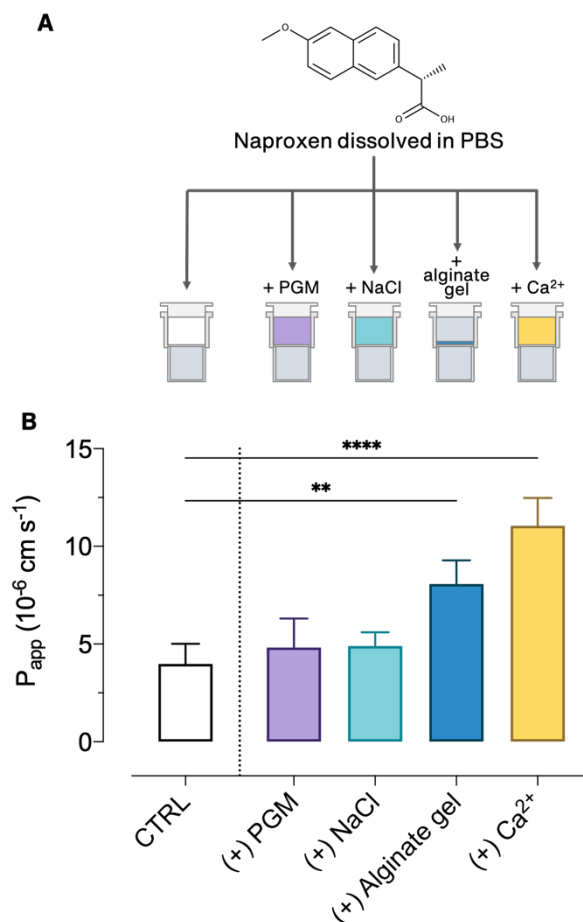
Figure 6. (A) The experimental setup used to isolate the effect of each one of the components of mucus. (B) the permeability of naproxen recorded in the presence of individual components of mucus.

3.4.2. The role of calcium

Once we isolated Ca^{2+} as the reason for the increased permeability, we then wanted to understand if this phenomenon is dependent on the negative charge borne by some of the drugs. Tests were repeated with ketoprofen and indomethacin as anions on which mucus increased their respective permeabilities, as well as $CFTR_{inh}$-172 and cefuroxime as anions with reduced and unvaried permeability (negative controls) in the presence of mucus, respectively. For naproxen, ketoprofen and indomethacin, permeability rises in presence of the alginate hydrogel and gets even higher in presence of the only $CaCl_2$ (Fig. 7A). It has been reported that these three drugs and other non-steroidal anti-inflammatory agents (NSAIDs) can form complexes with calcium[39–41]. Interestingly, Ogiso and colleagues reports that the absorption of indomethacin calcium salt on rat abdominal skin is significantly higher than that from indomethacin alone [41]. When forming complexes with calcium, naproxen, ketoprofen and indomethacin are neutralized; they shift from a negatively charged form to exhibiting no relative charge.

18

489   The neutralization implies a decrease of polarity in favor of lipophilicity which we think

490   it actually favors the diffusion through the artificial phospholipid membrane of PAMPA

491   (Fig. 7B). It should be noted, when drug-calcium complexes are formed, the molecular

492   descriptors are completely different from that of the free drugs and cannot be easily

493   calculated. In addition, the higher permeability observed with $CaCl_2$ could be due to

494   larger availability of free Ca^{2+} in solution. In fact, in the system containing alginate,

495   despite having the same Ca^{2+} concentration, part of it is not available because of the ion

496   crosslinking with alginate. On the contrary, we observe that the permeability of

497     $CFTR_{inh}$-172 and cefuroxime is not influenced by the presence of calcium, even though

498   if they are also considered anionic drugs.

499   Overall, we hypothesized that drug-calcium salts have higher passive diffusion rates

500   through the PAMPA phospholipid artificial membrane with respect to the not-

501   complexed drug. However, the formation of calcium salts is not merely dependent on

502   the negative charge as not all the anionic drugs included in the dataset enhanced
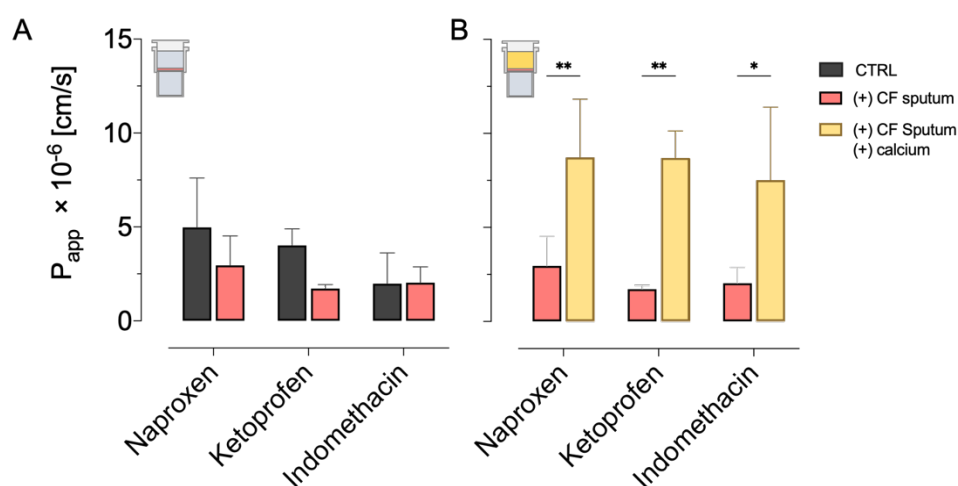
503   permeability.

504
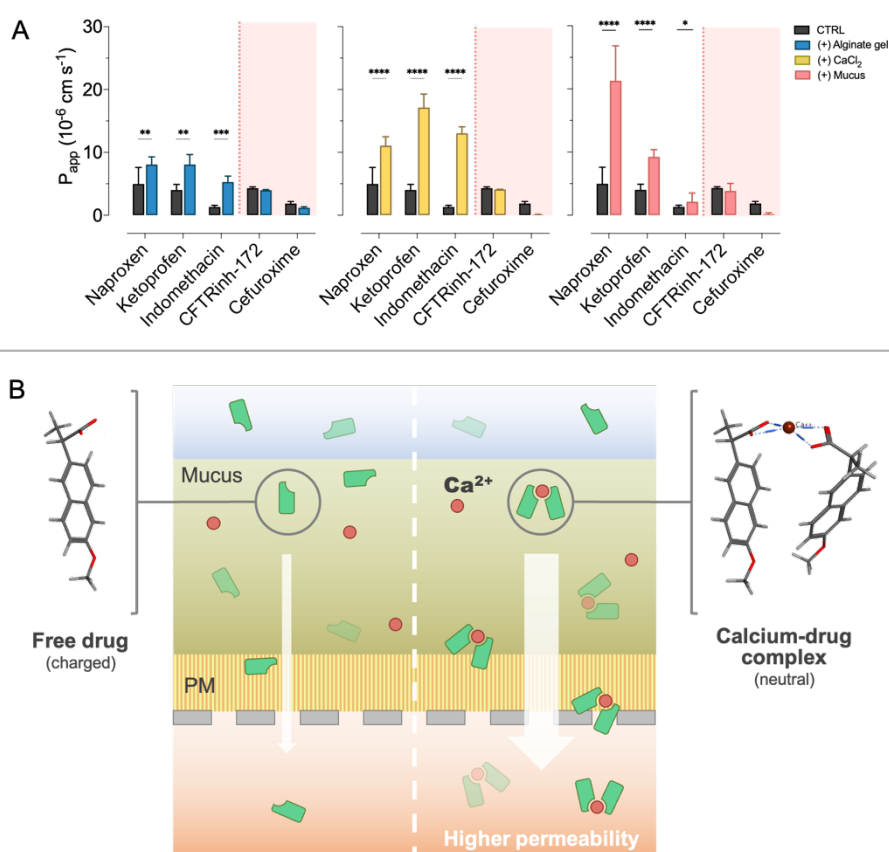
505
506

3.4.3. CF patient sputum validation

In the next step we wanted to understand if the results recorded in the presence of our mucus model can be reproduced using a more complex biological matrix to mimic CF sputum. For this purpose, we employed CF sputum as it is often considered a rough *ex vivo* model of CF mucus, and we measured the permeability of naproxen, ketoprofen and indomethacin. In fact, a hallmark of diseases such as CF, COPD and bronchiectasis is the excessive production of sputum. As a consequence of the altered physico-chemical properties, the diseased sputum contains higher concentrations of inflammatory mediators, lytic enzymes (*i.e.*, neutrophil elastase) and bacterial colonization. However, due to the high variability among patients, which depends on the diseases stage, the measurements performed with CF sputum may have a low reproducibility.

Given the high concentration of calcium in our mucus model we wanted to find out if the permeability of some negatively charged drugs results overestimated when using the mucus model developed by us. As expected, in the presence of the CF sputum the permeability of naproxen, ketoprofen and indomethacin was decreased, even though the variation was not statistically significant (FIG. 8A). Such a reduction could be the result of interactions with neutrophil elastase and proteases also present at high concentrations in the CF sputum. Mandel *et al.*[42], reported higher concentrations of calcium (136 ± 33 µg/mL) in submaxillary saliva of CF patients with respect to healthy people (71 ± 19 µg/mL). Based on these values, we can estimate almost a 10x higher concentration of calcium in our model than that of the *in vivo* scenario. Therefore, we can speculate that the permeability of some negatively charged drugs might be overestimated with our CF mucus model.

Despite this, we establish evidence indicating that some negatively charged drugs can form calcium-drug salts which have higher diffusion rates on PAMPA respect to the free drugs. In terms of permeability, these salts might be less affected by the barrier effect of mucus. Thus, we wondered if this mechanism can be exploited to increase the permeability of naproxen, ketoprofen and indomethacin through CF sputum. For this purpose, we repeated the permeability test through CF sputum, this time suspending the drugs into PBS containing calcium. As can be seen from Fig. 8B, the permeability of

544 all of the three drugs was significantly higher for the samples containing calcium. This

545 is likely a consequence of the formation of calcium complexes which increased more

546 than twice the permeability of the drugs through CF sputum.

547 Even though the concentration of calcium in the CF mucus is reported to be lower than

548 that of our mucus model, it is still clear the impact that calcium can play on permeability.

549 Drug calcium salts might have better biological activities and should be considered

550 when formulating drugs. For instance, high-dose ibuprofen taken constantly for years

551 has shown to significantly reduce the progression of the lung disease in cystic fibrosis[7].

552 It would be interesting to investigate if better health outcomes could be reached using

553 a calcium formulation.

554

555
556 Figure 8. The effect of calcium over the permeability of naproxen, ketoprofen and indomethacin in the
557 presence of cystic fibrosis (CF) sputum. (A) The permeability of the three drugs measured on the CF sputum
558 - PAMPA system and compared with PAMPA (CTRL). (B) The increase of permeability through the CF sputum
559 - PAMPA after the formation of calcium-drug complexes. Two way ANOVA was used to compute statistical
560 analysis.

561

562 **Conclusions**

563

564 Here we used an *in vitro* pathological cystic fibrosis mucus model to explore how it can

565 impact over permeability of a dataset of 45 compounds. Overall, our data suggest that

566 the activity of mucus is complex to predict. Determining the specific effects limiting the

567 permeability of drugs through mucus was out of the scope of this work. Yet, it was found

568 that the mucus was not only a physical barrier for the permeability of drugs but also

569 behaved as a dynamic filter as well. The permeability of most of the compounds was

570 reduced, whilst others have not been affected by the barriers of mucus. A poor

571 correlation of the effect of mucus on permeability was found for all of the selected
572 molecular descriptors. These findings represent an additional evidence of the further
573 need for reliable *in vitro* mucus models to be used for drug screening, especially in
574 mucus related disorders.
575 We also ascertained that calcium, which is one of the components of our mucus model,
576 enhanced the permeability of a small group of drugs. This was most likely the result of
577 the complexation with the drug. The observed increased-permeability effect induced
578 by calcium was also achieved also through cystic fibrosis sputum, further highlighting
579 the potential to use drugs as calcium salts to pursue higher absorption rates *in vivo*.
580 Additionally, calcium-based formulations could offer new potentialities also for the
581 repositioning of the current therapies.
582

583 **Declaration of competing interests**
584

585 The authors declare that they have no known competing financial interests or personal
586 relationships that could have appeared to influence the work reported in this paper.
587

592

593 **Abbreviations**
594

595 CF: cystic fibrosis
596 COPD: chronic obstructive pulmonary disease
597 PAMPA: parallel artificial membrane permeability assay.
598 PBS: phosphate buffer saline
599 HPLC-MS: high-pressure liquid chromatography – mass spectrometry
600 DMSO: dimethyl sulfoxide
601 P_{app}: apparent permeability
602 GDL: D-(+)-gluconic acid δ-lactone
603 MRM: multiple reaction monitoring
604 PCA: principal component analysis
605 Ro5: Lipinski rule of five
606 NSAID: non-steroidal anti-inflammatory drug

References

(1) Murgia, X.; Loretz, B.; Hartwig, O.; Hittinger, M.; Lehr, C. The Role of Mucus on Drug Transport and Its Potential to Affect Therapeutic Outcomes. *Adv. Drug Deliv. Rev.* **2018**, *124*, 82–97. https://doi.org/10.1016/j.addr.2017.10.009.

(2) Cone, R. A. Barrier Properties of Mucus. *Adv. Drug Deliv. Rev.* **2009**, *61* (2), 75–85. https://doi.org/10.1016/j.addr.2008.09.008.

(3) Fahy, J. V.; Dickey, B. F. Airway Mucus Function and Dysfunction. *N. Engl. J. Med.* **2010**, *363* (23), 2233–2247. https://doi.org/10.1056/nejmra0910061.

(4) Mitri, C.; Xu, Z.; Bardin, P.; Corvol, H.; Touqui, L.; Tabary, O. Novel Anti-Inflammatory Approaches for Cystic Fibrosis Lung Disease: Identification of Molecular Targets and Design of Innovative Therapies. *Front. Pharmacol.* **2020**, *11* (July), 1–25. https://doi.org/10.3389/fphar.2020.01096.

(5) Meldrum, O. W.; Chotirmall, S. H. Mucus, Microbiomes and Pulmonary Disease. *Biomedicines* **2021**, *9* (6), 675. https://doi.org/10.3390/biomedicines9060675.

(6) Murray, M. P.; Pentland, J. L.; Turnbull, K.; MacQuarrie, S.; Hill, A. T. Sputum Colour: A Useful Clinical Tool in Non-Cystic Fibrosis Bronchiectasis. *Eur. Respir. J.* **2008**, *34* (2), 361–364. https://doi.org/10.1183/09031936.00163208.

(7) Konstan, M. W.; Byard, P. J.; Hoppel, C. L.; Davis, P. B. Effect of High-Dose Ibuprofen in Patients with Cystic Fibrosis. *N. Engl. J. Med.* **1995**, *332* (13), 848–854. https://doi.org/10.1056/nejm199503303321303.

(8) Suk, J. S.; Lai, S. K.; Wang, Y. Y.; Ensign, L. M.; Zeitlin, P. L.; Boyle, M. P.; Hanes, J. The Penetration of Fresh Undiluted Sputum Expectorated by Cystic Fibrosis Patients by Non-Adhesive Polymer Nanoparticles. *Biomaterials* **2009**, *30* (13), 2591–2597. https://doi.org/10.1016/j.biomaterials.2008.12.076.

(9) Yu, T.; Chisholm, J.; Choi, W. J.; Anonuevo, A.; Pulicare, S.; Zhong, W.; Chen, M.; Fridley, C.; Lai, S. K.; Ensign, L. M.; Suk, J. S.; Hanes, J. Mucus-Penetrating Nanosuspensions for Enhanced Delivery of Poorly Soluble Drugs to Mucosal Surfaces. *Adv. Healthc. Mater.* **2016**, *5* (21), 2745–2750. https://doi.org/10.1002/adhm.201600599.

(10) Boegh, M.; Nielsen, H. M. Mucus as a Barrier to Drug Delivery - Understanding and Mimicking the Barrier Properties. *Basic Clin. Pharmacol. Toxicol.* **2015**, *116* (3), 179–186. https://doi.org/10.1111/bcpt.12342.

643   (11) Kansy, M.; Senner, F.; Gubernator, K. Screening : Parallel Artificial Membrane
644   Permeation Assay in the Description Of. *J. Med. Chem.* **1998**, *41* (7), 1007–
645   1010.

646   (12) Artursson, P.; Palm, K.; Luthman, K. Caco-2 Monolayers in Experimental and
647   Theoretical Predictions of Drug Transport. *Adv. Drug Deliv. Rev.* **2012**, *64*
648   (SUPPL.), 280–289. https://doi.org/10.1016/j.addr.2012.09.005.

649   (13) Di, L.; Whitney-Pickett, C.; Umland, J. P.; Zhang, H.; Zhang, X.; Gebhard, D. F.;
650   Lai, Y.; Federico III, J. J.; Davidson, R. E.; Smith, R.; Reyner, E. L.; Lee, C.; Feng, B.;
651   Rotter, C.; Varma, M. V; Kempshall, S.; Fenner, K.; El-kattan, A. F.; Liston, T. E.;
652   Troutman, M. D. Development of a New Permeability Assay Using Low-Efflux
653   MDCKII Cells. *J. Pharm. Sci.* **2011**, *100* (11), 4974–4985.
654   https://doi.org/10.1002/jps.22674.

655   (14) Sarmento, B. *Concepts and Models for Drug Permeability Studies - Cell and*
656   *Tissue Based In Vitro Culture Models*, 1st Editio.; Woodhead Publishing, 2015.

657   (15) Lock, J. Y.; Carlson, T. L.; Carrier, R. L. Mucus Models to Evaluate the Diffusion
658   of Drugs and Particles. *Adv. Drug Deliv. Rev.* **2018**, *124*, 34–49.
659   https://doi.org/10.1016/j.addr.2017.11.001.

660   (16) Butnarasu, C.; Barbero, N.; Pacheco, D.; Petrini, P.; Visentin, S. Mucin Binding to
661   Therapeutic Molecules: The Case of Antimicrobial Agents Used in Cystic
662   Fibrosis. *Int. J. Pharm.* **2019**, *564* (January), 136–144.
663   https://doi.org/10.1016/j.ijpharm.2019.04.032.

664   (17) Norris, D. A.; Sinko, P. J. Effect of Size, Surface Charge, and Hydrophobicity on
665   the Translocation of Polystyrene Microspheres through Gastrointestinal
666   Mucin. *J. Appl. Polym. Sci.* **1997**, *63* (11), 1481–1492.
667   https://doi.org/10.1002/(SICI)1097-4628(19970314)63:11<1481::AID-
668   APP10>3.0.CO;2-5.

669   (18) Boegh, M.; Baldursdóttir, S. G.; Müllertz, A.; Nielsen, H. M. Property Profiling of
670   Biosimilar Mucus in a Novel Mucus-Containing in Vitro Model for Assessment
671   of Intestinal Drug Absorption. *Eur. J. Pharm. Biopharm.* **2014**, *87* (2), 227–235.
672   https://doi.org/10.1016/j.ejpb.2014.01.001.

673   (19) Onnainty, R.; Usseglio, N.; Bonafé Allende, J. C.; Granero, G. Exploring a New
674   Free-Standing Polyelectrolyte (PEM) Thin Film as a Predictive Tool for Drug-
675   Mucin Interactions: Insights on Drug Transport through Mucosal Surfaces. *Int.*
676   *J. Pharm.* **2021**, *604* (March), 120764.
677   https://doi.org/10.1016/j.ijpharm.2021.120764.

678   (20) Grainger, C. I.; Greenwell, L. L.; Lockley, D. J.; Martin, G. P.; Forbes, B. Culture of

679   Calu-3 Cells at the Air Interface Provides a Representative Model of the Airway

680   Epithelial Barrier. *Pharm. Res.* **2006**, *23* (7), 1482–1490.

681   https://doi.org/10.1007/s11095-006-0255-0.

682 (21) Falavigna, M.; Klitgaard, M.; Brase, C.; Ternullo, S.; Škalko-Basnet, N.; Flaten, G.

683   E. Mucus-PVPA (Mucus Phospholipid Vesicle-Based Permeation Assay): An

684   Artificial Permeability Tool for Drug Screening and Formulation Development.

685   *Int. J. Pharm.* **2018**, *537* (1–2), 213–222.

686   https://doi.org/10.1016/j.ijpharm.2017.12.038.

687 (22) Pacheco, D. P.; Butnarasu, C. S.; Briatico Vangosa, F.; Pastorino, L.; Visai, L.;

688   Visentin, S.; Petrini, P. Disassembling the Complexity of Mucus Barriers to

689   Develop a Fast Screening Tool for Early Drug Discovery. *J. Mater. Chem. B*

690   **2019**, *7* (32), 4940–4952. https://doi.org/10.1039/C9TB00957D.

691 (23) Hentzer, M.; Teitzel, G. M.; Balzer, G. J.; Heydorn, A.; Molin, S.; Givskov, M.;

692   Parsek, M. R. Alginate Overproduction Affects Pseudomonas Aeruginosa

693   Biofilm Structure and Function. *J. Bacteriol.* **2001**, *183* (18), 5395–5401.

694   https://doi.org/10.1128/JB.183.18.5395-5401.2001.

695 (24) Leid, J. G.; Willson, C. J.; Shirtliff, M. E.; Hassett, D. J.; Parsek, M. R.; Jeffers, A. K.

696   The Exopolysaccharide Alginate Protects Pseudomonas Aeruginosa Biofilm

697   Bacteria from IFN-γ-Mediated Macrophage Killing . *J. Immunol.* **2005**, *175* (11),

698   7512–7518. https://doi.org/10.4049/jimmunol.175.11.7512.

699 (25) Bidmon, K.; Lieleg, O.; Berensmeier, S. An Optimized Purification Process for

700   Porcine Gastric Mucin with Preservation of Its Native Functional Properties.

701   *RSC Adv.* **2016**, *6*, 44932–44943. https://doi.org/10.1039/C6RA07424C.

702 (26) Wishart, D. S.; Knox, C.; Guo, A. C.; Shrivastava, S.; Hassanali, M.; Stothard, P.;

703   Chang, Z.; Woolsey, J. DrugBank: A Comprehensive Resource for in Silico Drug

704   Discovery and Exploration. *Nucleic Acids Res.* **2006**, *34* (Database issue), 668–

705   672. https://doi.org/10.1093/nar/gkj067.

706 (27) Kim, S.; Chen, J.; Cheng, T.; Gindulyte, A.; He, J.; He, S.; Li, Q.; Shoemaker, B. A.;

707   Thiessen, P. A.; Yu, B.; Zaslavsky, L.; Zhang, J.; Bolton, E. E. PubChem in 2021:

708   New Data Content and Improved Web Interfaces. *Nucleic Acids Res.* **2021**, *49*

709   (D1), D1388–D1395. https://doi.org/10.1093/nar/gkaa971.

710 (28) Sharifian Gh., M. Recent Experimental Developments in Studying Passive

711   Membrane Transport of Drug Molecules. *Mol. Pharm.* **2021**.

712   https://doi.org/10.1021/acs.molpharmaceut.1c00009.

713 (29) Oriano, M.; Terranova, L.; Sotgiu, G.; Saderi, L.; Bellofiore, A.; Retucci, M.;

714   Marotta, C.; Gramegna, A.; Miglietta, D.; Carnini, C.; Marchisio, P.; Chalmers, J.

715   D.; Aliberti, S.; Blasi, F. Evaluation of Active Neutrophil Elastase in Sputum of

716   Bronchiectasis and Cystic Fibrosis Patients: A Comparison among Different

717   Techniques. *Pulm. Pharmacol. Ther.* **2019**, *59* (October), 1–6.

718   https://doi.org/10.1016/j.pupt.2019.101856.

719   (30)   Chen, X.; Murawski, A.; Patel, K.; Crespi, C. L.; Balimane, P. V. A Novel Design of

720   Artificial Membrane for Improving the PAMPA Model. *Pharm. Res.* **2008**, *25*

721   (7), 1511–1520. https://doi.org/10.1007/s11095-007-9517-8.

722   (31)   Teixeira, L. de S.; Chagas, T. V.; Alonso, A.; Gonzalez-alvarez, I.; Bermejo, M.;

723   Polli, J.; Rezende, K. R. Biomimetic Artificial Membrane Permeability Assay

724   over Franz Cell Apparatus Using Bcs Model Drugs. *Pharmaceutics* **2020**, *12*

725   (10), 1–16. https://doi.org/10.3390/pharmaceutics12100988.

726   (32)   Sugano, K.; Takata, N.; Machida, M.; Saitoh, K.; Terada, K. Prediction of Passive

727   Intestinal Absorption Using Bio-Mimetic Artificial Membrane Permeation

728   Assay and the Paracellular Pathway Model. *Int. J. Pharm.* **2002**, *241* (2), 241–

729   251. https://doi.org/10.1016/S0378-5173(02)00240-5.

730   (33)   Artursson, P.; Bergström, C. A. S. Intestinal Absorption: The Role of Polar

731   Surface Area. *Drug Bioavailability*. May 27, 2003, pp 339–357.

732   https://doi.org/https://doi.org/10.1002/3527601473.ch15.

733   (34)   Di, L.; Kerns, E. H.; Fan, K.; McConnell, O. J.; Carter, G. T. High Throughput

734   Artificial Membrane Permeability Assay for Blood-Brain Barrier. *Eur. J. Med.*

735   *Chem.* **2003**, *38* (3), 223–232. https://doi.org/10.1016/S0223-

736   5234(03)00012-6.

737   (35)   Köllmer, M.; Mossahebi, P.; Sacharow, E.; Gorissen, S.; Gräfe, N.; Evers, D. H.;

738   Herbig, M. E. Investigation of the Compatibility of the Skin PAMPA Model with

739   Topical Formulation and Acceptor Media Additives Using Different Assay

740   Setups. *AAPS PharmSciTech* **2019**, *20* (2), 1–10.

741   https://doi.org/10.1208/s12249-019-1305-3.

742   (36)   Matsson, P.; Kihlberg, J. How Big Is Too Big for Cell Permeability? *J. Med. Chem.*

743   **2017**, *60* (5), 1662–1664. https://doi.org/10.1021/acs.jmedchem.7b00237.

744   (37)   Jamieson, C.; Moir, E. M.; Rankovic, Z.; Wishart, G. Structure-Brain Exposure

745   Relationships. *J. Med. Chem.* **2006**, *49* (17), 12–14.

746   https://doi.org/10.1021/jm060379l.

747   (38)   Shityakov, S.; Neuhaus, W.; Dandekar, T.; Förster, C. Analysing Molecular Polar

748   Surface Descriptors to Predict Blood-Brain Barrier Permeation. *Int. J. Comput.*

749   *Biol. Drug Des.* **2013**, *6* (1–2), 146–156.

750   https://doi.org/10.1504/IJCBDD.2013.052195.

751   (39)   Tang, B.; Wang, J.; Wang, Q.; Xiao, Y.; Huang, Y.; Liao, X.; Li, H. Calcium(II)–

752   Naproxen Complex: Synthesis, Characterization, and Interaction with Human

753   Serum Albumin. *Spectrosc. Lett.* **2016**, *49* (6), 404–412.

754   https://doi.org/10.1080/00387010.2016.1174137.

755   (40)   Atassi, F.; Mao, C.; Masadeh, A. S.; Byrn, S. R. Solid-State Characterization of

756   Amorphous and Mesomorphous Calcium Ketoprofen. *J. Pharm. Sci.* **2010**, *99*

757   (9), 3684–3697. https://doi.org/10.1002/jps.21925.

758   (41)   Ogiso, T.; Ito, Y.; Iwaki, M.; Atago, H. Absorption of Indomethacin and Its

759   Calcium Salt through Rat Skin: Effect of Penetration Enhancers and

760   Relationship between in Vivo and in Vitro Penetration. *J. Pharmacobiodyn.*

761   **1986**, *9*, 517–525.

762   (42)   Mandel, I. D.; Eriv, A.; Kutscher, A.; Denning, C.; Thompson, R. H.; Kessler, W.;

763   Zegarelli, E. Calcium and Phosphorus Levels in Submaxillary Saliva. *Clin.*

764   *Pediatr. (Phila).* **1969**, *8* (3), 161–164.

765   https://doi.org/10.1177/000992286900800308.

766